

Abstract:
 We study the temperature structure of chromospheric network fibrils using high-resolution observations from DKIST telescope. These first public release observations provide simultaneous photospheric and chromospheric spectra at high angular resolution. We use LTE and NLTE diagnostics to infer the temperature stratification in the fibrils and compare it with numerical simulations such as BIFROST.

Introduction:

1. Chromospheric fibrils: Thin elongated structures, exhibit wave dynamics, believed to be tracing low-lying horizontal B-field lines (de la Cruz Rodriguez & Socas-Navarro 2011).
2. Ca II 854.2nm spectral line forms in the lower-middle chromosphere, is an excellent diagnostic tool (Quintero Noda et al. 2016).
3. Thermodynamic properties of chromospheric fibrils important for modelling and understanding the mass and energy flows in the solar atmosphere.

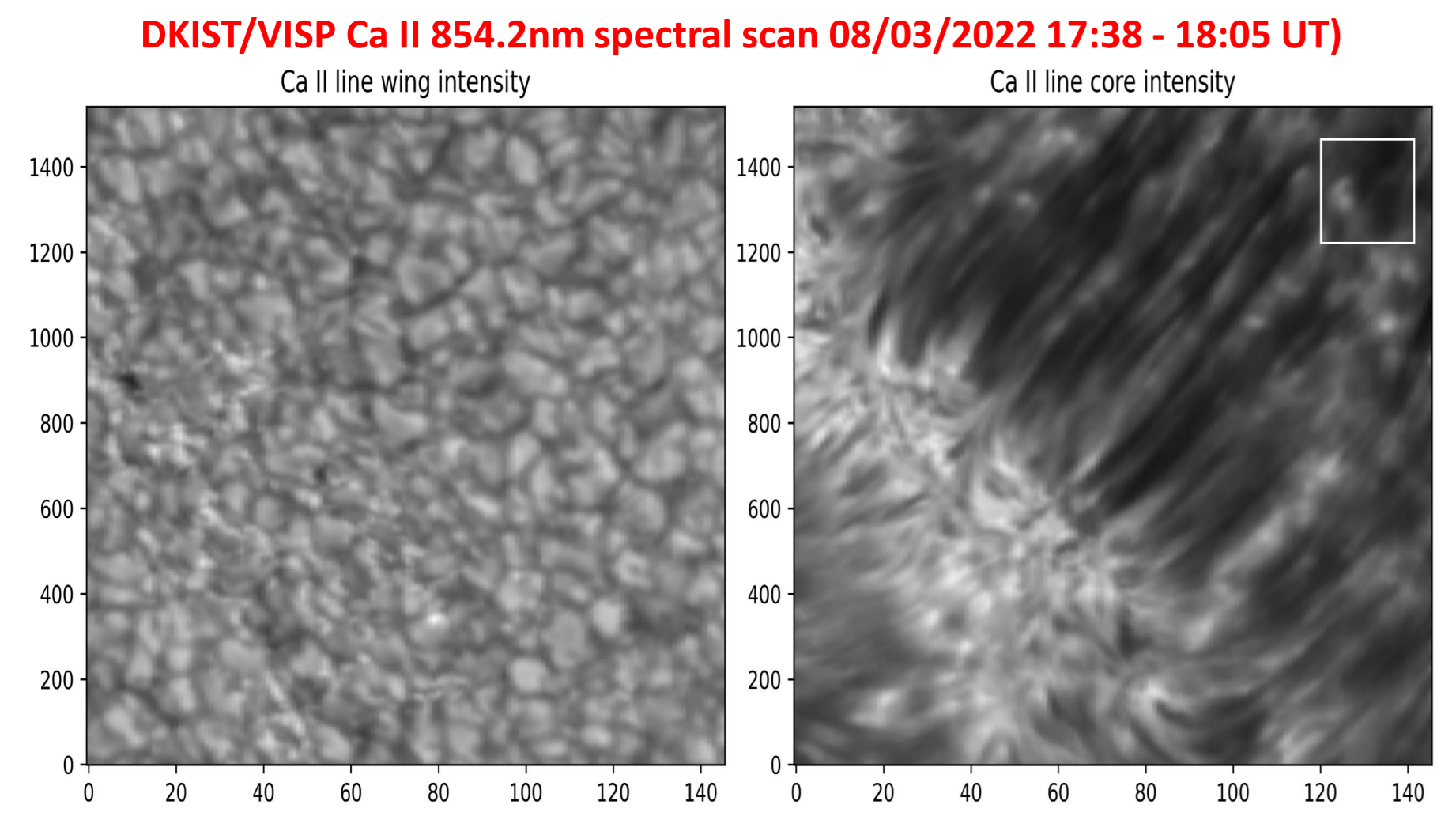


Figure 1: Left (Right) panel shows the wing (core) intensity map in Ca II 854 nm line, for a portion of the observed region. White rectangle on top-right corner of right panel represents region where quiet Sun profile for DKIST was averaged.

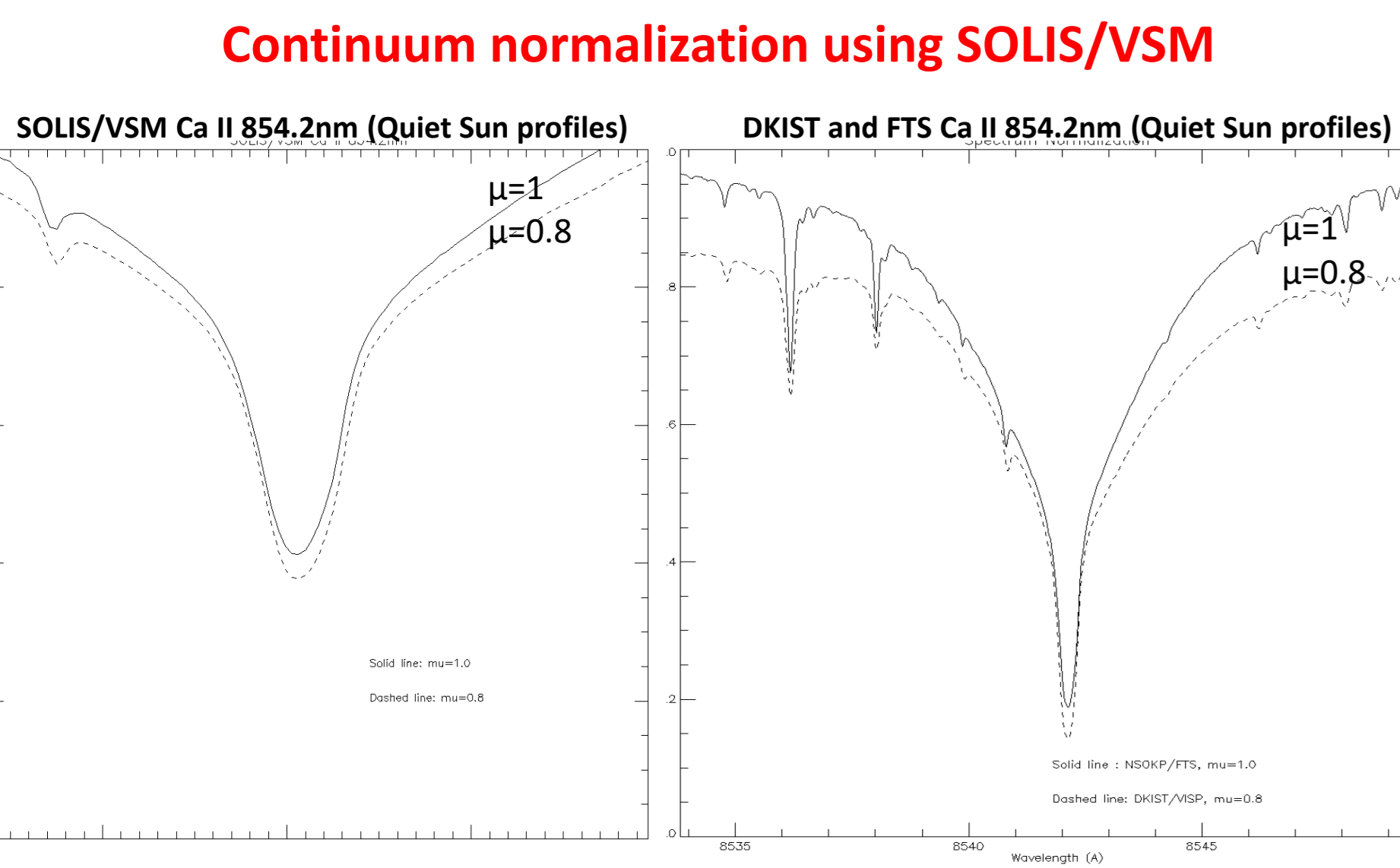


Figure 2: Left panel shows the Ca II 854 quiet sun spectrum at two different heliocentric angles ($\mu=1$; solid curve) and ($\mu=0.8$; dashed curve) derived from the full disk observations by SOLIS/VSM instrument (Keller 1998). Right panel shows similar profiles FTS ($\mu=1$) and DKIST ($\mu=0.8$) normalized in agreement with SOLIS/VSM as a reference. Wavelength scale and dispersion are computed using FTS spectral atlas (Neckels & Labs).

DKIST/VISP Observations:

- **Proposal:** ID 1_118 (public release)
- **Target:** Decaying plage region
- **Date:** August 3rd, 2022, 17:38 – 18:05 UT **Coordinates:** [-360°, -410°]
- **Spatial sampling:** 0.21" per pixel.
- **Temporal Cadence:** ~25 min
- **VBI:** G-band, Ca II K)
- **VISP:** Fe I 630 nm and Ca II 854 nm (simultaneous).
- **Polarimetry:** Full Stokes profiles (Not fully calibrated for crosstalk)

Data Processing:

- **Spectral Calibration:** Using NSO KittPeak FTS atlas the wavelength scale and dispersion was calibrated.
- **Continuum Normalization:** Using SOLIS/VSM full disk Ca II spectra (calibrated with FTS) the DKIST spectra were normalized for $\mu=0.8$.
- **Polarization:** Only Stokes-I information is used in this work.

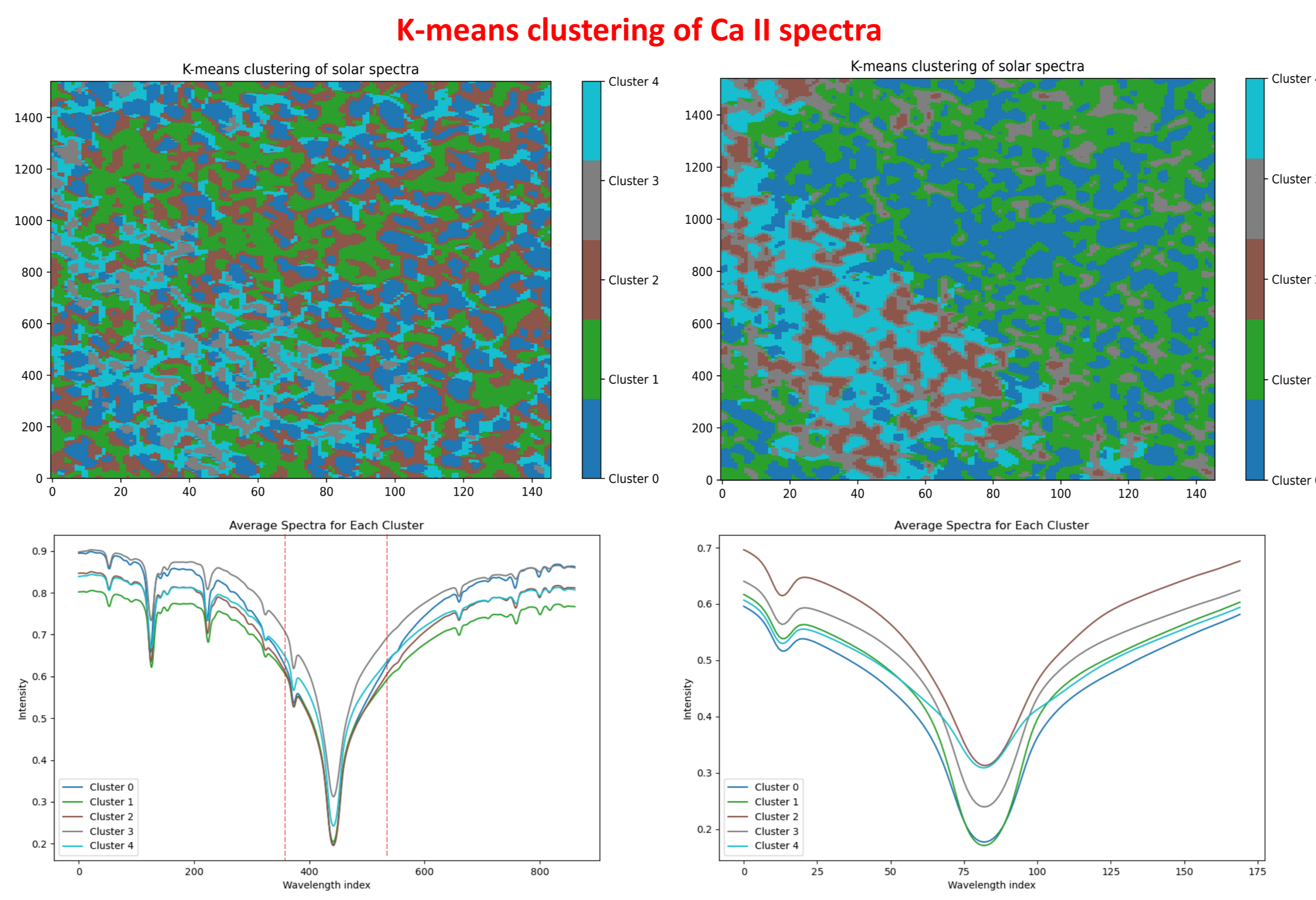


Figure 3: K-means clustering of the profiles into 5 clusters, color-coded in form of maps (top panels) and color-coded mean profile for each cluster (bottom panels), are shown for full spectral range (left) and limited spectral range near line core (right).

Data Analysis:
 NLTE inversion done pixel-by-pixel is a very slow process, a good guess model is thus necessary. We use following approaches for a good initialization.

- **Inversion Approach 1: K-means Clustering**
 - We group similar looking profiles in the selected field-of-view into 5 clusters or groups using an unsupervised machine learning technique called K-means clustering algorithm.
 - Clustering of profiles with full wavelength span leads to clustering of features which are dominated by line wing or continuum, such as granulation (See Figure 3, top left panel).
 - A narrow region near line core (dashed vertical red lines in bottom left panel of Figure 3) is selected for clustering. The results are shown in the top-right panel of Figure 3. They now show chromospheric features (plage and fibrils).
 - Mean spectra for each of the five clusters are shown in the bottom panels (each cluster is color coded in the displayed map and corresponding profiles).
 - The mean spectra has higher SNR due to averaging but may be broader due to velocities.
 - The five cluster spectra are inverted with a NLTE inversion code NICOLE (Socas-Navarro et al 2015) and results are shown in Figure 4.
 - Cluster#4 represents plage region and the corresponding inverted temperature model shows a significant enhancement of couple of thousand Kelvin in the optical depth range $\log \tau = -4$ to -6 .
 - The retrieved model atmospheres serve as good initial guess model for the corresponding cluster.
- **Inversion Approach 2: Database search of pre-computed profiles from BIFROST MHD models**
 - We use numerical MHD model of an enhanced network: BIFROST MHD simulation snapshot 385 (Gudiksen et al 2011, Carlsson et al 2016) to synthesize a database of Ca II Stokes-I spectra, using NICOLE code.
 - Then we match each spectra in DKIST observation to the synthetic spectra database and find a best match in the least square sense (Beck et al 2019) and pick the corresponding model atmosphere.
 - The maps of intensity in the wing and core of the Ca II line for the observations and the best-matched spectra in the database are shown in Figure 5. These show a good correspondence.
 - The map of mean temperature (between optical depths $\log \tau = -1.5$ to -4.5) from this database search approach is shown in Figure 6.
 - The mean temperature of the bright plage region is about 6 - 7 kK, while for the region with fibrils it is 4 – 4.5 kK, with the exception of a dark fibril and few other places which seems to be cool to about 3-4 kK.
 - This approach provides a good initial guess model for further pixel-by-pixel inversions, and is very fast (<1 minute). Such approach can provide for a quick-look analysis.

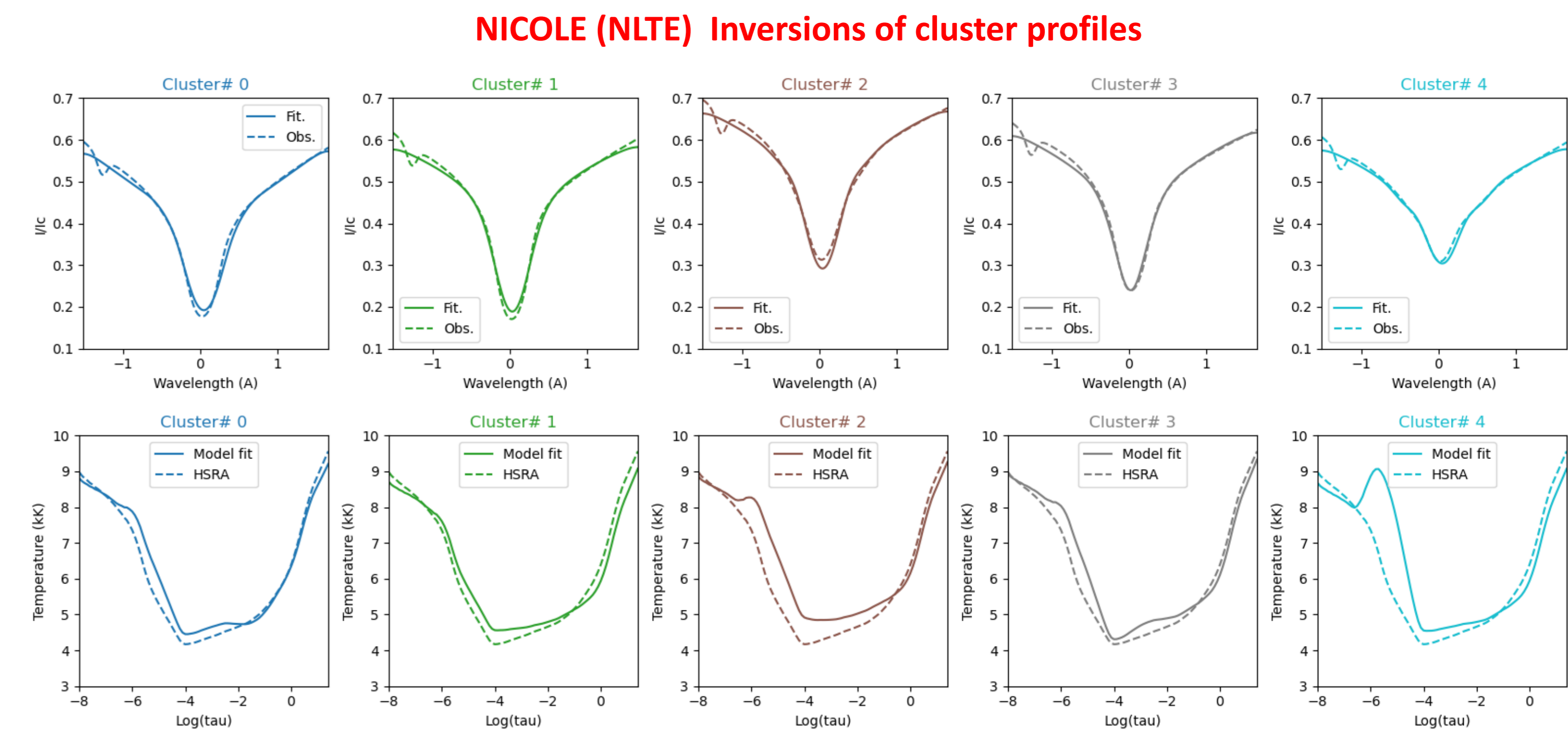


Figure 4: Top panels show mean spectra for each cluster (dashed) and best-fit spectra from NICOLE inversions. Bottom panels show the stratification of temperature with optical depth corresponding to the best fit model. Dashed curve is HSRA reference atmosphere.

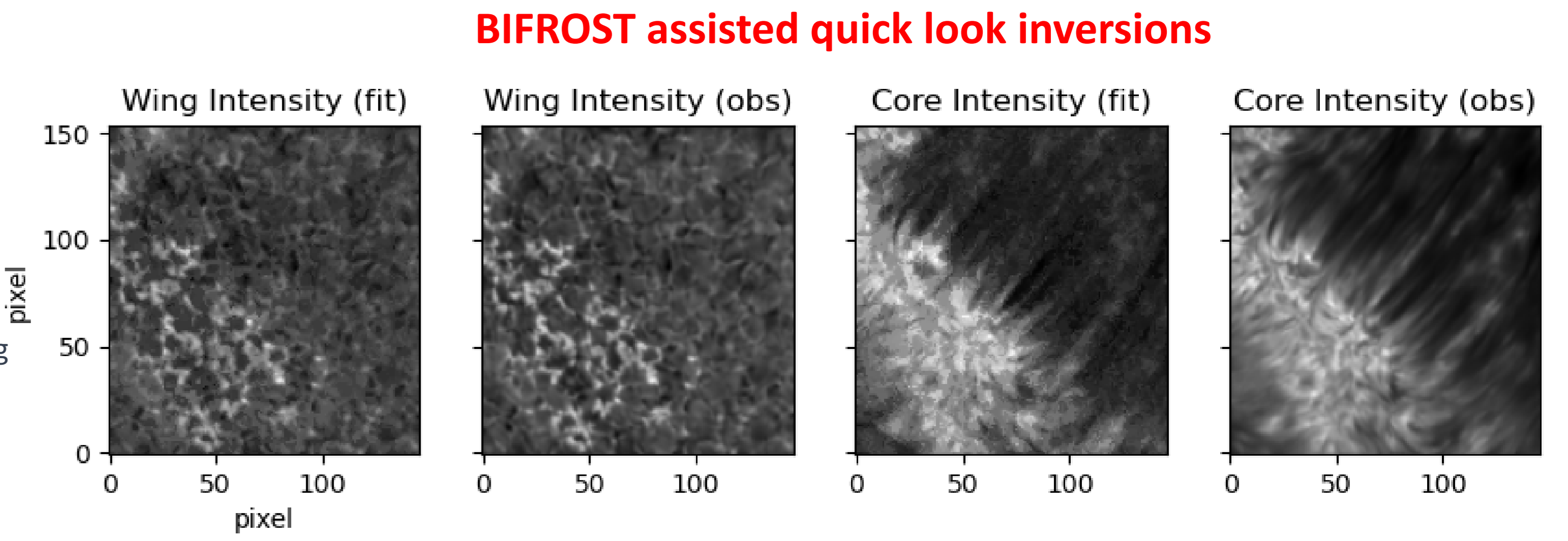


Figure 5: Inversion results from the database search approach are shown. The observed (fitted) intensity maps in the wing (left two panels) and the core of the Ca II line (right two panels) are shown.

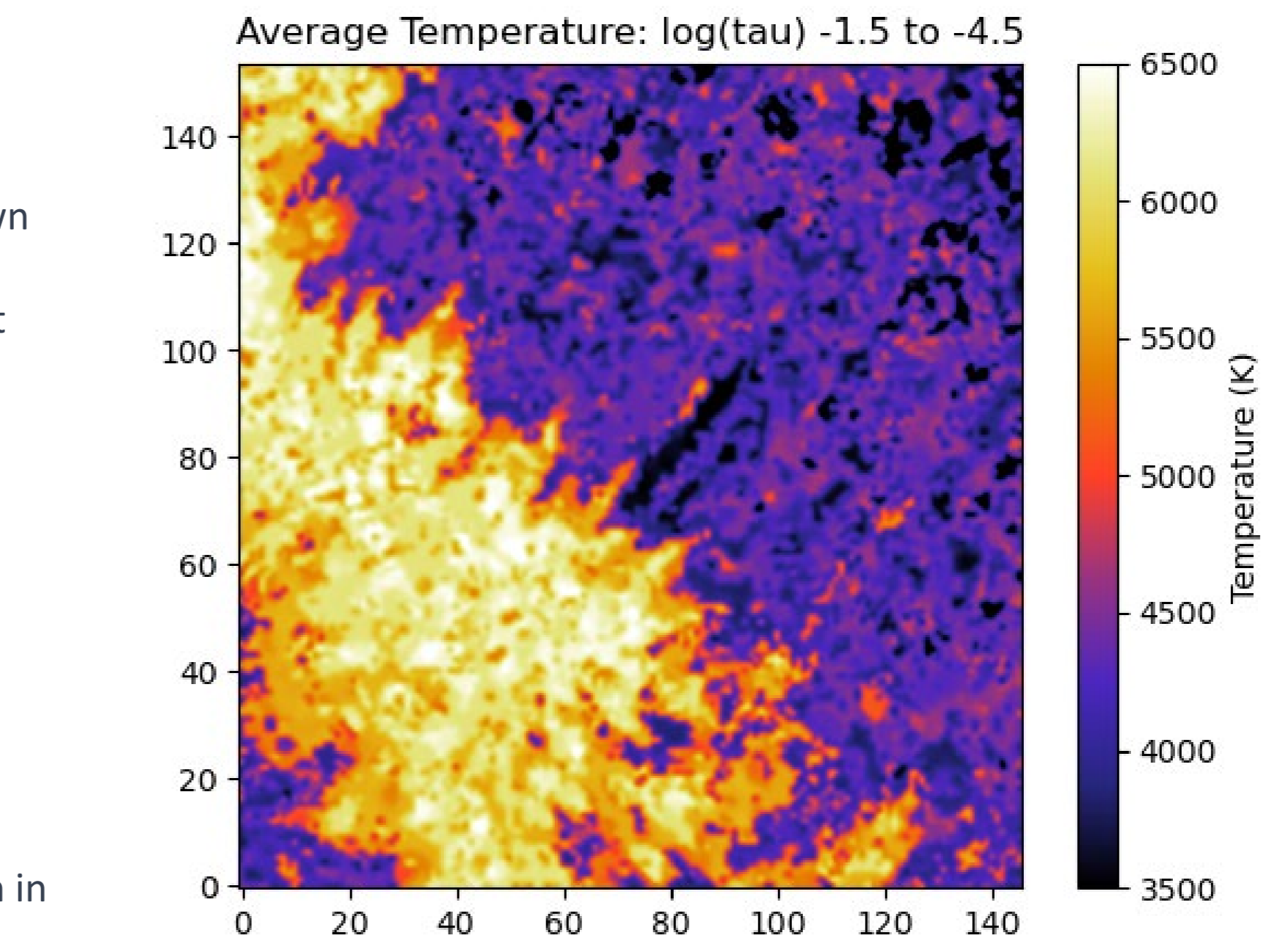


Figure 6: Map of mean temperature (averaged over optical depths $\log \tau = -1.5$ to -4.5), derived with database search approach is shown. Notice enhanced temperature in plage region as compared to fibril dominated region and a cool dark elongated fibril near the center of the map, oriented at 45 degrees.

References:

1. De Wijn, A et al., Solar Physics, 2022 DOI: 10.1007/s11207-022-01954-1
2. Carlsson, Mats et al, 2016 A&A 585, A4 (2016) DOI: 10.1051/0004-6361/201527226
3. Gudiksen, B. V., Carlsson, M., Hansteen, V. H., et al. 2011, A&A, 531, A154
4. Socas-Navarro, H, et al A&A 577, A7 (2015) DOI: 10.1051/0004-6361/201424860
5. Quintero Noda, C. et al MNRAS 459, 3363–3376 (2016)
6. de la Cruz Rodriguez, J., & Socas-Navarro, H. 2011, A&A, 527, L8
7. Beck, C. et al, ApJ, V 878, Issue 1, article id. 60, 15 pp. (2019).
8. Keller, C U, Proc. SPIE Vol. 3352, p. 732-741, 1998.